

A Rate - Dependent Elastic Plastic Constitutive Equation in Finite Deformation Based on a Slip Model

Yong-Yun Nam* · Sa-Soo Kim** · Sang-Gab Lee***

슬립모델을 이용한 변형률의존 유형변형 탄소성재료의 구성방정식 개발

남용운* · 김사수** · 이상갑***

< 目 次 >	
요 약 Abstract	4. Generalization of Plastic Development Equations
I. INTRODUCTION	IV. STRAIN RATE - DEPENDENT CONSTITUTIVE EQUATIONS
II. BASIC FRAMEWORK FOR THE CONSTITUTIVE EQUATIONS	V. MATERIAL CONSTANTS AND APPLICATION FOR UNIAXIAL TENSILE LOADING
III. STRIAN RATE - DEPENDENT PLASTIC DEVELOPMENT EQUATIONS	VI. CONCLUSION
1. Dislocative Velocity	REFERENCES
2. Dislocation Density	
3. Slip Velocoty	

요 약

최근들어 안전하고 합리적인 구조를 설계하기 위하여 구조물의 내충돌 또는 내충격에 대한 요구와 관심이 높아지고 있는데, 이러한 문제들은 아주 짧은 시간동안에 대변형이 일어나는 비선형문제라는 특징이 있다. 구조재료는 변형속도가 빨라짐에 따라 정적인 범주에서 보이는 거동과는 달리 변형률의존적인 거동을 보인다. 따라서 대변형 소성문제인 충돌해석 등에는 종래 사용하여 온 변형률 비의존 재료구성방정식으로는 한계가 있다.

이 논문에서는 이러한 점을 개선하기 위하여 연강의 소성거동을 잘 나타낼 수 있는 소성슬립모델을 채용하고, 비선형경화를 도입하여 변형도 적용범위를 확장한 대변형 탄소성 변형률의존 재료구성

* Institute of Fundamental Technological Research, Poland, Post - Doc.

** 부산대학교 조선공학과 교수

*** 한국해양대학교 조선공학과 조교수

방정식을 제시하였다. 본 구성방정식의 특징으로 항복조건과 하중조건이 필요없기 때문에 계산이 간편하며, 전위밀도와 속도로써 소성을 표현하기 때문에 보다 물리적인 의미를 가지고 금속재료의 소성현상을 나타낼 수 있다.

Abstract

The advanced development in many fields of engineering and science has caused many interests and demands for crashworthiness and non-linear dynamic transient analysis of structure response. Crash and impact problems have a dominant characteristic of large deformation for short time scales with material plasticity. The structural material shows rate-dependent behaviors in those cases. Conventional rate-independent constitutive equations used in the general purposed finite analysis programs are inadequate for dynamic finite strain problems.

In this paper, a rate-dependent constitutive equation for elastic-plastic material is developed. The plastic stretch rate is modeled based on slip model with dislocation velocity and its density so that there is no yielding condition, and no loading conditions. Non-linear hardening rule is also introduced for finite strain. Material constants of present constitutive equation are determined by experimental data of mild steel, and the constitutive equation is applied to uni-axial tension loading.

I. Introduction

In recent years, there has been a growing interest and demand in the crashworthiness of structures for the safe and reasonable design, which has a characteristic of the nonlinear problems involving large deformation over short time scales. From the end of 1970's, hydrocodes such as NIKED, DYNA2D, DYNA3D, DYTRAN, etc. have been developed for the numerical analysis of these problems. By the way, the structural materials show rate-dependent behaviors rather than rate-independent ones with increasing strain rate¹⁻³⁾. Therefore, conventional rate-independent constitutive equation has a limitation for the analysis of large deformation finite strain problem such as crash or impact analysis.

Perzyna⁴⁾ proposed Perzyna-type rate-dependent constitutive equation in 1963, introducing relaxation functions and drawing dynamic yield condition. On the other hand, Gilman⁵⁾ suggested Johnston-Gilman-type rate-dependent constitutive equation in 1965, using the model of dislocation velocity and dislocation density. Rice⁶⁾ established a theoretical framework of a flow potential for rate-dependent inelastic behavior in 1971. Recently, Paglietti⁷⁾ explained the elastoplastic

deformation based on the Bell's experimental results, by interpreting an elastic limit by the thermodynamic theory and by describing rate – dependent plastic deformation as the change of elastic limit. However, these models have not yet been arranged, and practical constitutive equations applied to these models have not been published.

Perzyna – type and Johnston – Gilman – type are usually used at present as the rate – dependent constitutive equations^{8 – 10}. That is because these types are convenient to approximate the experimental results of dislocation velocity to exponential rules¹¹. Since the exponential rules do not consider dislocation density, it is hard to apply these to mild steel in which the change of dislocation density sensitively affects the plastic deformation behavior. Though Johnston – Gilman – type constitutive equation is used, it has not yet been applied to hydrocodes, the range of its application is still narrow, and it is not generalized to apply to the general purpose finite element programs.

The objective of this paper is to develop large deformation, rate – dependent elastic plastic constitutive equation, by employing the slip model to represent well the plastic deformation behavior of mild steel for improvement of the above problems, and by introducing a nonlinear hardening to broaden an applicable range of strain. The others are to develop the computational algorithm applicable to the finite element programs and hydrocodes, and to enable to analyze more reasonably large deformation, dynamic plastic problem such as collision and stranding of ship. Mild steel is the object of the developed constitutive equation here, body – centered cubic lattice material is also possible to be applied to.

I . BASIC FRAMEWORK FOR THE CONSTITUTIVE EQUATIONS

Assuming elastic and plastic deformations to be non – ductile, Helmholtz free energy can be composed of the elastic and plastic terms as follows :

$$\psi(\mathbf{E}_e, H_1, H_k) = \psi_e(\mathbf{E}_e) + \psi_p(H_1, H_k) \quad (2.1)$$

where \mathbf{E}_e is Green strain tensor, H_1 and H_k are the internal variables indicating isotropic hardening and kinematic hardening, respectively. Assume that the fourth order tensor, constant, C_{ijkl} is introduced, and that the elastic free energy can be expressed as follows :

$$\rho\psi_e(\mathbf{E}_e) = \frac{1}{2} \mathbf{E}_e : \mathbf{C} : \mathbf{E}_e \quad (2.2)$$

Since Green strain tensor \mathbf{E}_e and the 2nd Piola – Kirchhoff stress $\boldsymbol{\sigma}_p$ are conjugate, the 2nd Piola – Kirchhoff stress can be described as follows :

$$\sigma_p = \rho \frac{\partial \psi_e}{\partial \mathbf{E}_e} = \mathbf{C} : \mathbf{E}_e \quad (2.3)$$

Differentiating Eq. (2.3) with time, the following incremental form can be obtained :

$$\dot{\sigma}_p = \mathbf{C} : \dot{\mathbf{E}}_e \quad (2.4)$$

Since the 2nd Piola - Kirchhoff stress and Green strain are the Lagrangian tensors, their differentiations with time also satisfy objectivity. The tensor field from Eq. (2.4), therefore, is objective.

When Eq. (2.4) is expressed as Eulerian tensor after its transformation, stress rate becomes objective. Pre - and post - multiplying both sides of Eq. (2.4) with deformation gradient tensor leads to the following :

$$\frac{1}{J} \mathbf{F} \dot{\sigma}_p \mathbf{F}^T = \frac{1}{J} \mathbf{F} \mathbf{C} : \dot{\mathbf{E}}_e \mathbf{F}^T \quad (2.5)$$

The left side of above Eq. (2.5) is Truesdel rate, $\dot{\sigma}^T$. The right side of Eq. (2.5) is developed as follows :

$$\frac{1}{J} \mathbf{F} \mathbf{C} : \dot{\mathbf{E}}_e \mathbf{F}^T = \frac{1}{J} \text{tr}(\mathbf{C} \mathbf{F}^T \dot{\mathbf{E}}_e \mathbf{F}^T) = \mathbf{C} : \frac{1}{J} \mathbf{F}^T \dot{\mathbf{E}}_e \mathbf{F}^T = \mathbf{C} : \frac{1}{J} \mathbf{F}_p^T (\mathbf{F}_e^T)^2 \mathbf{D}_e \mathbf{F}_e \mathbf{F}_p^T \mathbf{F}_e^T \quad (2.6)$$

Assuming the updated Lagrangian method, then $J \doteq 1$, $\mathbf{F}_p = \mathbf{F}_e = \mathbf{F} \doteq \mathbf{I}$. Stretch rate tensor, therefore, can be used as the strain rate. Eqs. (2.5) and (2.6) can, therefore, be expressed as follows :

$$\dot{\sigma}^T = \mathbf{C} : \mathbf{D}_e = \mathbf{C} : (\mathbf{D} - \mathbf{D}_p) \quad (2.7)$$

where \mathbf{D} , \mathbf{D}_e and \mathbf{D}_p are total, elastic and plastic stretch rate tensors, respectively.

III. STRAIN RATE - DEPENDENT PLASTIC DEVELOPMENT EQUATIONS

1. Dislocation Velocity

Johnston¹²⁾ examined the dislocation velocity and its density in Lif closely through experiments. The dislocation velocity showed to be extremely sensitive to applied stress. The following four models for the dislocation velocity are usually used : exponential type model approximated from experimental results for the dislocation velocity, velocity model from the point defect drag, model based on the thermal excitation, and model based on the friction and dispersion of phonon at high strain rate. In this study, the point defect drag model such as the following expression is used, which is suitable for body - centered cubic lattice material :

$$\mathbf{v} = v_0 e^{\tau/D} \quad (3.1)$$

where v_0 is a limiting velocity of dislocation, D is a characteristic drag stress, and τ is a applied shear stress.

2. Dislocation Density

The growth of dislocation is also sensitive to applied stress. When a dislocation is subjected to a constant stress that is sufficiently high to make it multiply, the density of loops along its glide plane increases with time¹³⁾. The number of dislocations increases exponentially with time at the beginning of the multiplication process. This density within the band begins to increase only after the surface of the crystal is completely covered with glide bands. The lateral growth of the glide bands is a linear function of the macroscopic strain.

It is verified the dislocation density (the number of dislocation per area) increases almost linearly up to 10% with strain in Lif. Johnston¹⁴⁾ modeled the change of the dislocation density based on this fact. If δ is the number of new dislocation loops per length of wake, then the rate of change of number of loops is as follow :

$$dN = 2\delta N dx \quad (3.2)$$

where dx is a linear distance swept out by each dislocation, and $dx = v dt$. Integration of Eq. (3.2) with time gives

$$N = N_0 e^{2\delta v t} \quad (3.3)$$

Eq. (3.3) means that the total number of loops in a growing band increases exponentially with time, and represents one - dimensional slip. Since attrition of dislocation occurs in addition to multiplication during growth of a three - dimensional glide band, the overall rate change of dislocation density ρ is written as

$$\frac{d\rho}{dt} = \alpha\rho - \beta\rho^2 \quad (3.4)$$

3. Slip Velocity

Slip velocity is affected by the dislocation velocity and the dislocation density, that is, slip is determined by the number of dislocations and their velocities. Slip velocity can be represented by the dislocation velocity and its density as following procedure. When a dislocation moves along the distance x_i , slip δ_i can be written as

$$\delta_1 = \frac{x_1}{l} b \quad (3.5)$$

where b is the Burgers vector. If a dislocation moves along the length l , a slip proceeds by the Burgers vector. Therefore, slip velocity is described as

$$\dot{\gamma}_1 = \frac{v_1}{l} b \quad (3.6)$$

where v_1 is a dislocation velocity. Assuming there are N dislocations on slip plan, Eq. (3.6) is rearranged as follows :

$$\dot{\gamma} = \rho b v \quad (3.7)$$

where v is the average dislocation velocity and $\rho = N/l$.

It is reported that dislocations are composed of the edge and screw components, and that the edge components move about 50 times as fast as the screw components at a given stress[12]. Considering this point, Eq. (3.7) can be modified as follow :

$$\dot{\gamma} = b(\rho_e v_e + \rho_s v_s) \quad (3.8)$$

where the subscripts, e and s , refer to the edge and screw dislocations, respectively. Using $\rho_s/\rho_e = v_e/v_s \approx 50$ and $\rho = \rho_s + \rho_e \approx \rho_s$, Eq. (3.8) may be written as

$$\dot{\gamma} = b\rho_s v_s \left(1 + \frac{\rho_s v_s}{\rho_s v_s}\right) \approx 2b\rho_s v_s \approx 2b\rho v_s \quad (3.9)$$

Finally, slip velocity $\dot{\gamma}$ is expressed in terms of the dislocation density and the dislocation velocity as shown in Eq. (3.9). Slip velocity of Eq. (3.9) can be obtained when the dislocation density and the dislocation velocity are expressed by the stress and the slip.

Gilman⁵⁾ derived the dislocation density from Eqs. (3.4) and (3.9). Setting $\beta=0$ of Eq. (3.4), combination of this with Eq. (3.9) yields

$$\rho(\gamma) = (\rho_0 + \rho_1 \gamma) \quad (3.10)$$

This result is consistent with the experimental observation that the dislocation density increases linearly at the beginning of deformation. As straining proceeds, by the way, some of the dislocations of Eq. (3.10) will lose their mobility through several reasons and will become restrained dislocations. Their fraction also increases with increasing strain. If f is the fraction of the mobile dislocations, the expression for the change of f is as follow⁵⁾ :

$$df = -\phi f d\gamma \quad (3.11)$$

where ϕ is a coefficient. From Eq. (3.11), the fraction of the mobile dislocations f can be written as

$$f = e^{-\phi\gamma} \quad (3.12)$$

By combining Eqs. (3.10) and (3.12), the mobile dislocation density is then obtained as

$$\rho(\gamma) = (\rho_o + \rho_1\gamma)e^{-\phi\gamma} \quad (3.13)$$

where ρ_o and ρ_1 are the initial dislocation density and the multiplication constant, respectively. From Eqs. (3.1) and (3.13), therefore, slip velocity is given by

$$\dot{\gamma} = 2bv_o(\rho_o + \rho_1\gamma)e^{-(\phi\gamma + \frac{H_o}{\tau})} \quad (3.14)$$

where ϕ decreases the slip velocity with increasing slip, which represents a kind of work – hardening. Letting $\phi = H_1/\tau$, then Eq. (3.14) can be written as

$$\dot{\gamma} = 2bv_o(\rho_o + \rho_1\gamma)e^{-\frac{H_o + H_1\gamma}{\tau}} \quad (3.15)$$

Since the real power necessary to move dislocations is the effective stress except the back stress (the long range stress) τ_b , the correction of Eq. (3.15) gives as follows :

$$\dot{\gamma} = 2bv_o(\rho_o + \rho_1\gamma)e^{-(\phi\gamma + \frac{H_o}{\tau})} \quad (3.16)$$

where the back stress represents a kinematic – hardening phenomena known as Bausinger's effect.

4. Generalization of Plastic Development Equations

In this study, the Johnston – Gilman – type constitutive equation is more generalized and is developed suitable for the large deformation, plastic expressions. Using the slip model explained previously, the plastic stretch rate tensor \mathbf{D}_p , the objective strain rate, is expressed as follows :

$$\mathbf{D}_p = C_o(\rho_o + \rho_1\tilde{\mathbf{E}}_p)\text{EXP}\left\{\frac{H_o + H + H_1\tilde{\mathbf{E}}_p}{(\sqrt{J_2(\boldsymbol{\sigma} - \mathbf{B}')}})}\right\} \frac{\boldsymbol{\sigma} - \mathbf{B}'}{\sqrt{J_2(\boldsymbol{\sigma} - \mathbf{B}')}} \quad (3.17)$$

where \mathbf{B} is the back stress representing the Bausinger's effect. To model the plastic deformation within the longer range of deformation rate, the exponential term governing the deformation rate for the stress is modified as follows :

$$\text{EXP} \left\{ \frac{H_0^n + H(\sqrt{J_2}(\boldsymbol{\sigma}' - \mathbf{B}'))^{n-1} + H_1 \tilde{E}_p (\sqrt{J_2}(\boldsymbol{\sigma}' - \mathbf{B}'))^{n-1}}{(\sqrt{J_2}(\boldsymbol{\sigma}' - \mathbf{B}'))^n} \right\} \quad (3.18)$$

where, H_0 , n and H_1 are the material constants, \mathbf{B}' is deviatoric back stress, \tilde{E}_p is an accumulated plastic deformation, H is a hardening function defined in the following Eq. (3.19), and $J_2(\boldsymbol{\sigma}' - \mathbf{B}')$ is the second invariant of the effective stress $(\boldsymbol{\sigma}' - \mathbf{B}')$. In the above equation, whereas the back stress represents kinematic hardening, H_1 and H , isotropic hardening. n and H_0 govern dynamic yield stresses of material.

The constitutive equation is completed obtaining the development equations for the hardening and back stress in Eq. (3.18), and the constants are determined from the experimental results. The functions of back stress and isotropic hardening are modeled as follows, based on the hardening model of Hu¹⁵⁾ :

$$\dot{H} = C_p (H_s - H) \tilde{D}_p \quad (3.19)$$

$$\dot{\mathbf{B}} = C_b \left(\frac{1}{2} \left(1 + \frac{H}{H_s} \right) B_s \mathbf{D}_p - \mathbf{B} \tilde{D}_p \right) \quad (3.20)$$

where C_p , H_s , C_b , B_s are the material constants from experiments, \tilde{D}_p is the equivalent strain rate as follows :

$$\tilde{D}_p = \sqrt{\frac{1}{2} \mathbf{D}_p : \mathbf{D}_p} \quad (3.21)$$

IV. Strain Rate - Dependent Constitutive Equations

The constitutive equation of elastoplastic materials explained up to the present is rearranged. Constitutive equation is largely made up of the relationship of objective stress and strain (2.7), plastic development equations (3.17) and (3.18), and equations for hardening and back stress (3.19) and (3.20). Especially, there are no yielding condition and loading /unloading condition in these plastic development equations, rather than the rate - independent ones. The above equations are rearranged for convenience in Table 4.1.

In this study, midpoint rule is employed as time integration of constitutive equation which is arranged in the following Tables 4.2 and 4.3.

Table 4.1 Constitutive equation set

$\dot{\boldsymbol{\sigma}}^T = \mathbf{C} : (\mathbf{D} - \mathbf{D}_p)$
$\mathbf{D}_p = C_o (\rho_0 + \rho_1 \tilde{E}_p) \text{EXP} \left[\frac{H_0^n + H \mu^{n-1} + H_1 \tilde{E}_p \mu^{n-1}}{\mu^n} \right] \frac{(\boldsymbol{\sigma}' - \mathbf{B}')}{\mu}$
$\dot{H} = C_p (H_s - H) \tilde{D}_p$
$\dot{\mathbf{B}} = C_b \left(\frac{1}{2} \left(1 + \frac{H}{H_s} \right) B_s \mathbf{D}_p - \mathbf{B} \tilde{D}_p \right), \text{ where } \mu = \sqrt{J_2}$

Table 4.2 Time integration of constitutive equation by midpoint rule

STEP 0 : Calculate $\Delta \mathbf{u}$
STEP 1: $\mathbf{F}_n = \frac{\partial(\mathbf{x}_n + \Delta \mathbf{u})}{\partial \mathbf{x}_n} = \mathbf{I} + \frac{\partial(\Delta \mathbf{u})}{\partial \mathbf{x}_n}$
STEP 2: $\mathbf{L}_{n+\alpha} = \frac{\frac{1}{\Delta t} \left(\frac{\partial \Delta \mathbf{u}}{\partial \mathbf{x}_n} \right)}{\mathbf{I} + \alpha \left(\frac{\partial \Delta \mathbf{u}}{\partial \mathbf{x}_n} \right)}, \alpha = 0.5$
STEP 3: $\boldsymbol{\sigma}'_{n+\alpha} = \boldsymbol{\sigma}_n - \alpha \Delta t (\mathbf{L}_{n+\alpha} \boldsymbol{\sigma}_n + \boldsymbol{\sigma}_n \mathbf{L}_{n+\alpha}^T + \text{tr}(\mathbf{L}_{n+\alpha}) \boldsymbol{\sigma}_n)$
STEP 4: $\mathbf{D}_{n+\alpha} = \frac{1}{2} (\mathbf{L}_{n+\alpha} + \mathbf{L}_{n+\alpha}^T)$
STEP 5: Go to Table 4.3
STEP 6: $\hat{\boldsymbol{\sigma}}_{n+\alpha}^T = \mathbf{C} : (\mathbf{D}_{n+\alpha} - \mathbf{D}_p)$
STEP 7: $\boldsymbol{\sigma}_{n+\alpha} = \boldsymbol{\sigma}'_{n+\alpha} + \Delta t \hat{\boldsymbol{\sigma}}_{n+\alpha}^T$
STEP 8: $\boldsymbol{\sigma}_{n+1} = \boldsymbol{\sigma}_{n+\alpha} - (1 - \alpha) \Delta t (\mathbf{L}_{n+\alpha} \boldsymbol{\sigma}_{n+\alpha} + \boldsymbol{\sigma}_{n+\alpha} \mathbf{L}_{n+\alpha}^T + \text{tr}(\mathbf{L}_{n+\alpha}) \boldsymbol{\sigma}_{n+\alpha})$
STEP 9: Go to STEP 0

Table 4.3 Calculation of plastic stretch rate tensor

STEP 0: $\mathbf{E}'_{n+\alpha} = \mathbf{E}_n - \alpha \Delta t (\mathbf{L}_{n+\alpha} \mathbf{E}_n + \mathbf{E}_n \mathbf{L}_{n+\alpha}^T + \text{tr}(\mathbf{L}_{n+\alpha}) \mathbf{E}_n)$
$\mathbf{E}^p_{n+\alpha} = \mathbf{E}_n^p - \alpha \Delta t (\mathbf{L}_{n+\alpha} \mathbf{E}_n^T + \mathbf{E}_n^p \mathbf{L}_{n+\alpha}^T + \text{tr}(\mathbf{L}_{n+\alpha}) \mathbf{E}_n^p)$
$\mathbf{B}'_{n+\alpha} = \mathbf{B}_n - \alpha \Delta t (\mathbf{L}_{n+\alpha} \mathbf{B}_n + \mathbf{B}_n \mathbf{L}_{n+\alpha}^T + \text{tr}(\mathbf{L}_{n+\alpha}) \mathbf{B}_n)$
STEP 1: $P_\sigma = -\frac{1}{3} \text{tr}(\boldsymbol{\alpha}_{ij}), P_B = -\frac{1}{3} \text{tr}(\mathbf{B}_{ij})$ (Spherical Stress)
$\boldsymbol{\alpha}_{ij} = \boldsymbol{\sigma}_{ij} + P_\sigma \delta_{ij}, \mathbf{B}_{ij} = \mathbf{B}_{ij} + P_B \delta_{ij}$ (Deviatoric Stress)
STEP 2: $\mathbf{D}_p = C_o (\rho_b + \rho_l \tilde{\mathbf{E}}_n^p) \text{EXP} \left[\frac{H_o^n + H(\mu_{n+\alpha})^{n-1} + H_l \tilde{\mathbf{E}}_n^p (\mu_{n+\alpha})^{n-1}}{(\mu_{n+\alpha})^n} \right] \frac{\boldsymbol{\sigma}'_{n+\alpha} - \mathbf{B}'_{n+\alpha}}{\mu_{n+\alpha}}$
STEP 3: $\dot{H} = C_p (H_s - H) \dot{\mathbf{D}}_p$
STEP 4: $\dot{\mathbf{B}} = C_b \left(\frac{1}{2} \left(1 + \frac{H}{H_s} \right) \mathbf{B}_s \mathbf{D}_p - \mathbf{B} \dot{\mathbf{D}}_p \right)$
STEP 5: $\mathbf{E}_{n+\alpha} = \mathbf{E}'_{n+\alpha} + \Delta t \mathbf{D}_{n+\alpha}$
$\mathbf{E}^p_{n+\alpha} = \mathbf{E}^p_{n+\alpha} + \Delta t \mathbf{D}_p$
STEP 6: $\mathbf{E}_{n+1} = \mathbf{E}_{n+\alpha} - (1 - \alpha) \Delta t (\mathbf{L}_{n+\alpha} \mathbf{E}_{n+\alpha} + \mathbf{E}_{n+\alpha} \mathbf{L}_{n+\alpha}^T + \text{tr}(\mathbf{L}_{n+\alpha}) \mathbf{E}_{n+\alpha})$
$\mathbf{E}^p_{n+1} = \mathbf{E}^p_{n+\alpha} - (1 - \alpha) \Delta t (\mathbf{L}_{n+\alpha} \mathbf{E}^p_{n+\alpha} + \mathbf{E}^p_{n+\alpha} \mathbf{L}_{n+\alpha}^T + \text{tr}(\mathbf{L}_{n+\alpha}) \mathbf{E}^p_{n+\alpha})$
STEP 7: $\mathbf{B}_{n+\alpha} = \mathbf{B}'_{n+\alpha} + \Delta t \dot{\mathbf{B}}$
STEP 8: $\mathbf{B}_{n+1} = \mathbf{B}_{n+\alpha} - (1 - \alpha) \Delta t (\mathbf{L}_{n+\alpha} \mathbf{B}_{n+\alpha} + \mathbf{B}_{n+\alpha} \mathbf{L}_{n+\alpha}^T + \text{tr}(\mathbf{L}_{n+\alpha}) \mathbf{B}_{n+\alpha})$
$H_{n+1} = H_n + \Delta t \dot{H}$
STEP 9: $\dot{\mathbf{D}}_p = \sqrt{\frac{1}{2} \mathbf{D}_p : \mathbf{D}_p}$
STEP 10: $\tilde{\mathbf{E}}_{n+1}^p = \tilde{\mathbf{E}}_n^p + \Delta t \dot{\mathbf{D}}_p$
STEP 11: Go to SETP 6 of Table 4.2

V. MATERIAL CONSTANTS AND APPLICATION FOR UNIAXIAL TENSILE LOADING

Material constants are referred to mild steel S41C and are based on the Kuriyama's experiment²⁾. Fig. 5.1 shows the result of this experiment, rearranging and plotting true stress and true strain diagram. It is found that the upper and lower yield points occur and their difference increases with increasing strain rate as shown in Fig. 5.1. Macroscopic softening of material occurs around at 20% strain under static loading and at 9% strain under high strain rate. Softening means the material unstability, and this unstable phenomenon is concerned with the formation of slip band and its behavior. The material constants from Fig. 5.1 list at Table 5.1 within strain range between 0% and 15% except unstable region.

From Table 5.1, C_0 is material constant designated as $C_0=2bv$, where b is Burgers vector and v is limit dislocation velocity. Since $b=2.5 \times 10^{-7}$ mm and $v=3.2 \times 10^6$ mm/s in the case of mild steel, $C_0=1.6$ mm²/s. Material property ρ_1 representing the growth of dislocation density with plastic deformation is given by 10^9 mm⁻² in mild steel⁶⁾. Material properties C_0 and ρ_1 are fixed values in this material constitutive equation. The other material constants are determined by the experimental results. Since material constants n and H_0 control the yield stress, they are determined referring to the yield stress from stress -

Table 5.1 Material constants

C_0	1.6mm ² /s	ρ_1	10^9 mm ⁻²
n	1.35	H_0	50kg/mm ²
H_0	160kg/mm ²	B_0	30kg/mm ²
ρ_0	3.75×10^2 mm ⁻²	C_1	70
C_b	70	H_1	1200kg/mm ²

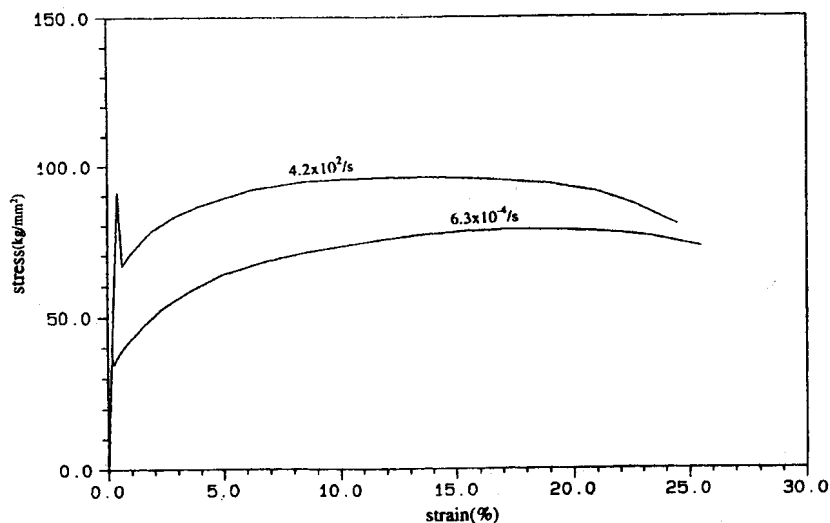


Fig. 5.1 Strain - stress curve of Kuriyama's experiment

strain diagram. The others are decided from the stress - strain diagram after yielding, because their properties control the material behavior after yielding.

To examine the applicability of this constitutive equation, the case of uniaxial tensile loading is applied. Fig. 5.2 shows the computational results of this constitutive equation and the Kuriyama's experimental results together, in which it can be seen that computational results realize the upper and lower yield points well and describe the experimental data well between 0% and 15% strain range. Here the strain rate is the one for the nominal strain. Fig. 5.3 represents the computational

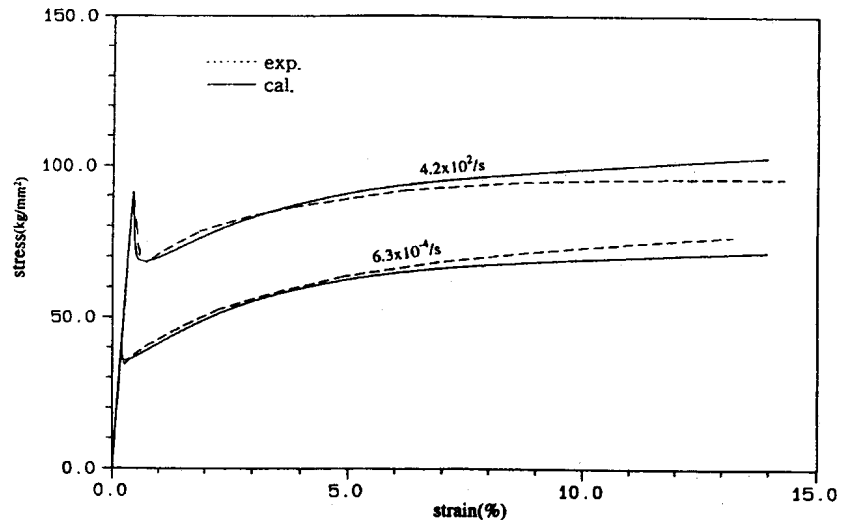


Fig. 5.2 Experimental and calculated strain - stress curve

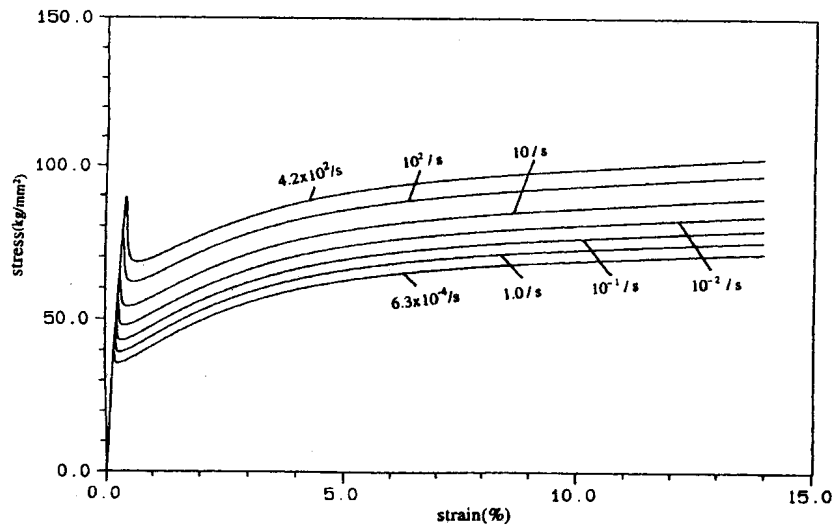


Fig. 5.3 Strain - stress curve according to strain rates

results of the yield stress and the flow stress for the strain rate in the range of strain rate between $6.3 \times 10^{-4}/s$ and $4.2 \times 10^2/s$. As shown in this figure, the present constitutive equation represents the strain rate dependence of mild steel well.

Figs. 5.4 and 5.5 show the change of the stress curves during loading when the strain rate is changed. Whereas Fig. 5.4 is the case of the strain rate increase from $6.3 \times 10^{-4}/s$ to $4.2 \times 10^2/s$ where dot line is the computational data of $4.2 \times 10^2/s$, Fig. 5.5 is the one of the strain rate decrease from $4.2 \times 10^2/s$ to $20/s$ where dot line is the experimental result. Generally, there is a phenomenon

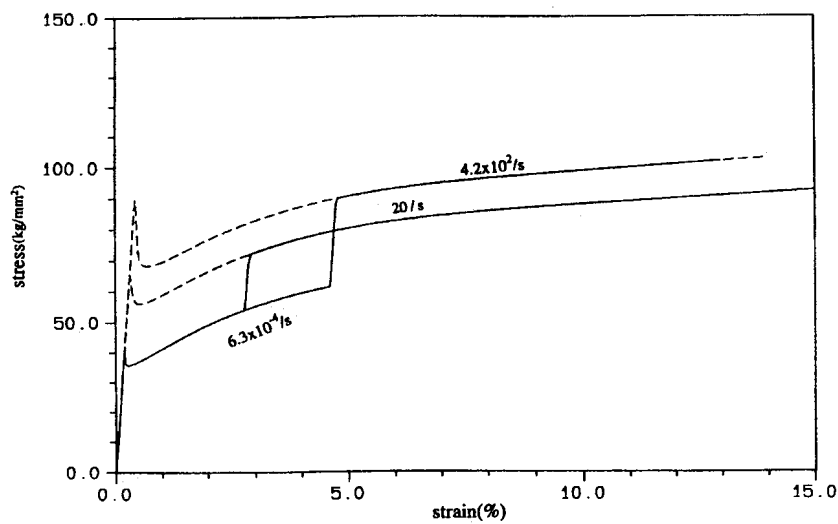


Fig. 5.4 Strain - stress curve for the change of strain rate during deformation (high rate after low rate)

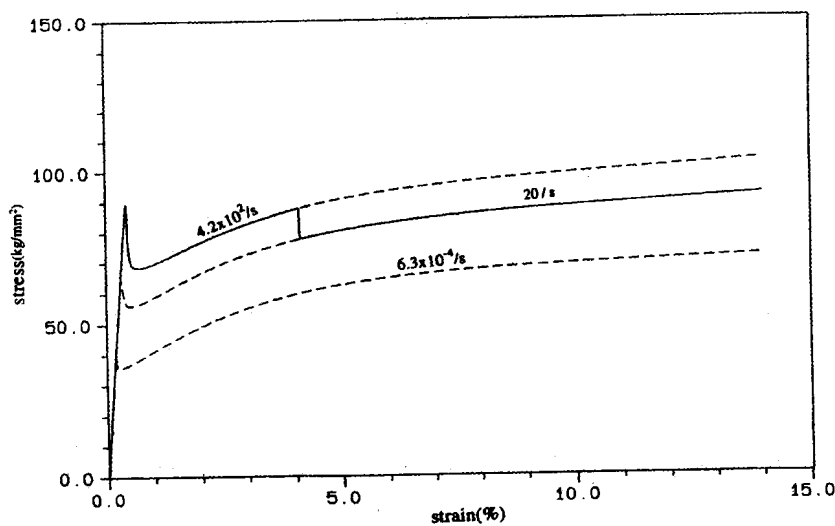


Fig. 5.5 Strain - stress curve for the change of strain rate during deformation (low rate after high rate)

of memory effect in material. The memory effect is that the past deformation history affects the present material behavior. While there is apparent memory effect in material such as aluminum, it is too small to be neglected in steel. The outer appearance effect of memory effect is usually represented by the gradual approach of the stress curve with changed strain rate during deformation to the previous one with unchanged strain rate. The present constitutive equation does not show this behavior as shown in Figs. 5.4 and 5.5. Therefore, it might be thought that this constitutive equation reasonably simulates the behavior of steel with the least memory effect.

VI. CONCLUSION

Using plastic development equation by the slip model expressed by the dislocation velocity and its density, the rate - dependent elastic plastic constitutive equation was developed, in which the applicable range of strain rate and strain was broadened by introducing exponential rule and non-linear hardening based on Johnston - Gilman - type. Yield and loading conditions are not needed as the special features of this constitutive equation, the calculation, therefore, is more convenient. Since plasticity is expressed by the dislocation velocity and its density, a plastic phenomenon of steel material can be expressed with more physical meanings.

As the results of the application of the developed constitutive equation to notably rate - dependent mild steel S41C, rate - dependence of mild steel is well represented. Because of wide applicable range of strain, the present constitutive equation can be applied to the dynamic plastic problems, hydrocodes and the general elastoplastic analysis programs, and may be enable reasonably to analyze the problems such as the collision and stranding of ship etc. Though mild steel is the object material here, body - centered cubic lattice material can usually be applicable to.

REFERENCES

- 1) Ulric S. Lindhdm(editor), Mechanical Behavior of Material Under Dynamic Loads, Spring - Verlag, 1968.
- 2) K. Kawata, S. Hasimoto and Kanayama, "A New Testing Method for the Characterisation Materials in High - Velocity Tension", *Mechanical Properties of Materials at High Rates of Strain*, 1979.
- 3) J. Harding(editor), Mechanical Properties of Materials at High Rates of Strain, Spring - Verlag, 1989.
- 4) Piotr Prezyna, "The Constitutive Equation for Rate Sensitive Plastic Materials", *Quarterly Journal of Applied Mathematics*, Vol. 20, No. 4, pp. 321 - 332, 1963.
- 5) J. J. Gilman, "Microdynamics of Plastic Flow at Constant Stress", *Journal of Applied Physics*, Vol. 9, pp. 2772 - 2777, 1965.
- 6) J. R. Rice, "Inelastic Constitutive Relation for Solids : An Internal Variable Theory and Its Application to Metal Plasticity", *J. Mech. Phys. Solids*, Vol. 19, pp. 433 - 455, 1971.
- 7) A. Paglietti, Thermodynamic nature and control of the elastic limit in solids, *International Journal of Non -*

Linear Mechanics, Vol. 24, No. 6, pp. 571 - 583, 1989.

- 8) S. Kuriyama and Kawata, "Propagation of Stress Wave with Plastic Deformation in Metal Obeying the Constitutive Equation of the Johnston - Gilman Type", *Journal of Applied Physics*, Vol. 44, No. 8, pp. 3445 - 3454, Aug. 1973.
- 9) S. R. Bodner. "Constitutive Equation for Elastic - Viscoplastic Strain - Hardening Materials", *ASME Journal of Applied Mechanics*, Vol. 42, pp. 385 - 389, June. 1975.
- 10) L. M. Taylor and E. B. Becker, "Some Computational Aspects of Large Deformation, Rate - Dependent Plasticity Problem", *Computer Methods in Applied Mechanics and Engineering*, Vol. 41, pp. 251 - 277, 1983.
- 11) S. Nemat - Nasser and D.T. Chung, "Phenomenological Modeling of Rate - Dependent Plasticity for High Strain Rate Problem", *Mechanics of Materials*, Vol. 7, pp. 319 - 344, 1989.
- 12) W. G. Johnston and J. J. Gilman, "Dislocation Velocities, Dislocation Densities, and Plastic Flow in Lithium Fluoride Crystals", *Journal of Applied Physics*, Vol. 30, No. 2, pp. 129 - 144, Feb. 1959.
- 13) J. J. Gilman, "Dislocation Mobility in Crystals", *Journal of Applied Physics*, Vol. 36, No. 10, pp. 3195 - 3206, 1965.
- 14) W. G. Johnston, "Yield Point and Delay Times in Single Crystals", *Journal of Applied Physics*, Vol. 33, No. 9, pp. 2716 - 2730, 1962.
- 15) Zaiqian Hu, Edgar Fernand Rauch and Cristian Teodosius, "Work - Hardening Behavior of Mild Steel Under Stress Reversal at Large Strains", *International Journal of Plasticity*, Vol. 8, pp. 839 - 856. 1992.